Topological Summation of Observables Measured with Dynamical Overlap Fermions

Wolfgang Bietenholz[*]

John von Neumann Institut für Computing NIC
Deutsches Elektron-Synchrotron DESY
Platanenallee 6
15738 Zeuthen, Germany
E-mail: bietenho@ifh.de

Ivan Hip

Faculty of Geotechnical Engineering
University of Zagreb
Hallerova aleja 7
42000 Varaždin, Croatia
E-mail: ivan.hip@gmail.com

HMC histories for light dynamical overlap fermions tend to stay in a fixed topological sector for many trajectories, so that the different sectors are not sampled properly. Therefore the suitable summation of observables, which have been measured in separate sectors, is a major challenge. We explore several techniques for this issue, based on data for the chiral condensate and the (analogue of the) pion mass in the 2-flavour Schwinger model with dynamical overlap-hypercube fermions.

---

[*]Speaker.

1. The 2-flavour Schwinger model

The Schwinger model (QED$_2$) on a Euclidean plane is characterised by the Lagrangian

$$\mathscr{L}(\bar{\Psi}, \Psi, A_\mu) = \bar{\Psi}(x)\left[\gamma_\mu(\mathrm{i}\partial_\mu + gA_\mu) + m\right]\Psi(x) + \frac{1}{2}F_{\mu\nu}(x)F_{\mu\nu}(x) \ . \tag{1.1}$$

Analytic results are obtained in the bosonised form, *e.g.* for the chiral condensate $\Sigma = -\langle\bar{\Psi}\Psi\rangle$ and the "meson" masses (iso-triplet and iso-singlet), with two degenerate flavours of mass $m \ll g$,

$$\Sigma(m) = 0.388\ldots(mg^2)^{1/3} \ \ [1] \ , \quad M_\pi = 2.008\ldots(m^2g)^{1/3} \ \ [1] \ , \quad M_\eta = \sqrt{\frac{2g^2}{\pi} + M_\pi^2} \ \ [2] \ . \tag{1.2}$$

Here we consider a lattice formulation with compact link variables $U_{\mu,x} \in U(1)$ and the plaquette gauge action. For the fermions we use the overlap-hypercube Dirac operator [3, 4]

$$D_{\mathrm{ovHF}} = (1 - \frac{m}{2})D_{\mathrm{ovHF}}^{(0)} + m \ , \quad D_{\mathrm{ovHF}}^{(0)} = 1 + (D_{\mathrm{HF}} - 1)/\sqrt{(D_{\mathrm{HF}}^\dagger - 1)(D_{\mathrm{HF}} - 1)} \ . \tag{1.3}$$

D_{HF} is a truncated perfect hypercube fermion operator, which is γ_5-Hermitian, $D_{\mathrm{HF}}^\dagger = \gamma_5 D_{\mathrm{HF}}\gamma_5$. Due to the use of the overlap formula [5] in eq. (1.3), $D_{\mathrm{ovHF}}^{(0)}$ solves the Ginsparg-Wilson relation in its simplest form [6], $\{D_{\mathrm{ovHF}}^{(0)}, \gamma_5\} = 2D_{\mathrm{ovHF}}^{(0)}\gamma_5 D_{\mathrm{ovHF}}^{(0)}$, which implies a lattice modified, exact chiral symmetry [7]. It reproduces the axial anomaly correctly in all topological sectors [8].

In the free case D_{HF} is discussed in Refs. [3, 4] (we refer to the version denoted as CO-HF). It is approximately chiral already, hence it changes only little in the transition to the overlap operator,

$$D_{\mathrm{HF}} \approx D_{\mathrm{ovHF}} \ , \tag{1.4}$$

in contrast to the Wilson kernel, which is used in the standard overlap operator [5]. Further virtues of D_{HF}, which are based on the renormalisation group construction, like improved scaling and approximate rotation symmetry are essentially inherited by D_{ovHF}. Also long-range couplings are only turned on slightly, again due to the similarity (1.4), which strongly improves the degree of locality compared to the standard overlap operator. As a related property, the condition number of the operator in the inverse square root of eq. (1.3) is strongly reduced.

The form of $D_{\mathrm{ovHF}}[U]$ interacting through $U(1)$ gauge fields was introduced in Ref. [4]. All the above virtues were tested and confirmed extensively for the 2-flavour Schwinger model. In that case, the configurations were generated quenched, but their contributions to the measurements were re-weighted with the fermion determinant [4, 9]. Also in quenched QCD, a drastically improved locality and approximate rotation symmetry have been confirmed for $D_{\mathrm{ovHF}}[U]$ [10].

2. Simulation with dynamical overlap fermions

Hybrid Monte Carlo (HMC) simulations with chiral fermions are tedious and still at an early stage. However, in addition to the virtues listed above, the property (1.4) also facilitates HMC simulations: a low polynomial in D_{HF} can be used for the HMC force and for short trajectories a useful acceptance rate persists [11, 12] (in the extreme case of using directly D_{HF}, however, its volume dependence was considered unsatisfactory [13]).

We performed HMC simulations with dynamical overlap-hypercube fermions at $\beta = 1/g^2 = 5$ on $L \times L$ lattices with two fermion flavours of mass m, where L and m take the following values:

$$\underline{L = 16} : m = 0.01 , \ 0.03 , \ 0.06 , \ 0.09 , \ 0.12 , \ 0.18 , \ 0.24 .$$

$$\underline{m = 0.01} : L = 16 , \ 20 , \ 24 , \ 28 , \ 32 .$$

We did not study a continuum extrapolation, but the lattices are fine (plaquette values ≈ 0.9), so we rely on small lattice artifacts (moreover $O(a)$ scaling artifacts are ruled out since we are using Ginsparg-Wilson fermions).

Our algorithm fulfils the conceptual conditions like detailed balance and area conservation [11]. The essential practical question is the acceptance rate in the Metropolis step at the end of the HMC trajectories (it employs $D_{\rm ovHF}$ to precision 10^{-16}). For $L = 16$ with trajectory length $\ell = 1/8$ we obtained acceptance rates in the range $0.3 \dots 0.5$, with only a mild dependence on the fermion mass [11]. In Figure 1 we show the dependence on the lattice size L at very light mass $m = 0.01$. The trajectory length is decreased for $L = 16$, 20, 24, 28, 32 to $\ell = 0.125$, 0.0625, 0.05, 0.04, 0.03, respectively. This keeps the acceptance rates in the same range, and large statistics allows for a selection of well decorrelated configurations.

A major challenge for the simulation with light dynamical overlap fermions — in addition to the huge computation time request in QCD — is that the histories at weak gauge coupling perform only very few topological transitions (which require a temporary deformation to rough configurations). We refer to the clean definition, which identifies the topological charge with the fermionic index ν [6]. In all our considerations only the absolute value $|\nu|$ matters.
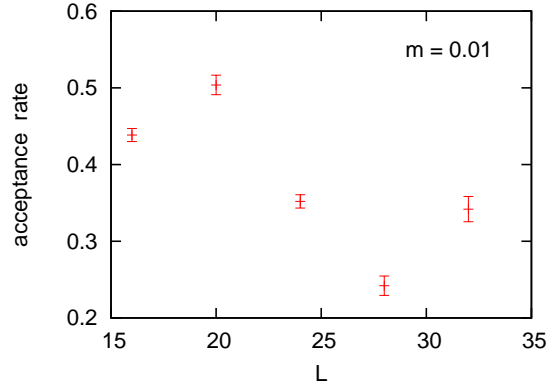
Figure 1: The acceptance rate of the HMC trajectories at $m = 0.01$ as a function of the lattice size L. Note that the trajectory length is reduced for increasing volume.
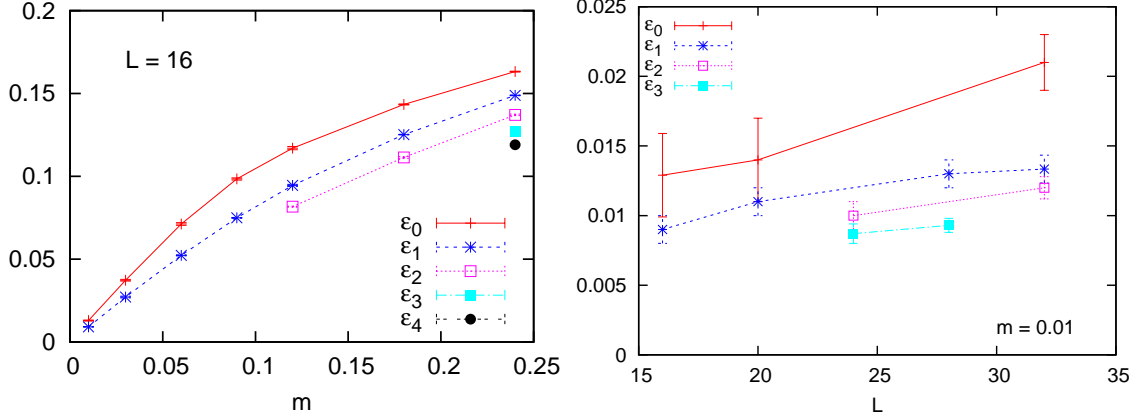
3. The chiral condensate Σ

For a configuration in volume $V = L^2$, the chiral condensate is given by

$$\Sigma = \frac{1}{V} \sum_i \frac{1}{|\lambda_i| + m} := \frac{|\nu|}{mV} + \varepsilon_{|\nu|} . \tag{3.1}$$

λ_i are the Dirac eigenvalues mapped stereographically onto the imaginary axis, $\lambda_i \to \lambda_i/(1 - \lambda_i/2)$, and the sum runs over all of them. The last term defines the quantity $\varepsilon_{|\nu|}$.

In Ref. [14] we discussed the determination of Σ based on the lowest non-zero eigenvalues and Random Matrix Theory (RMT). Since $\Sigma(m = 0) = 0$, this is not the setting that RMT usually refers to, so we are probing *terra incognita*. In fact we observed microscopic eigenvalue densities, which are not described by any known RMT formula. Nevertheless, the RMT interpretation of the ratio $\langle \lambda_1 \rangle_{\nu=0}/\langle \lambda_1 \rangle_{|\nu|=1}$ yields results for Σ, which agree well with the predicted value (1.2) over a broad parameter range. ($\langle \dots \rangle_{|\nu|}$ denotes an expectation value restricted to configurations of charge $|\nu|$.)

Here we address the *direct* measurement of Σ based on the full Dirac spectrum. Our results are shown in Figure 2. At small masses m, the zero mode contribution strongly dominates for

Figure 2: The contributions of the non-zero modes to the chiral condensate, $\varepsilon_{|\nu|}$, measured in the topological sectors $\pm \nu$. We show the mass dependence at $L = 16$ (left) and the lattice size dependence at $m = 0.01$ (right).

topologically charged configurations, so that the term $\varepsilon_{|\nu|}$ is a minor correction. As a generic property of stochastic Hermitian operators (such as $\gamma_5 D_{\text{ovHF}}$), zero modes repel low lying non-zero modes, which implies the hierarchy

$$\varepsilon_0 > \varepsilon_1 > \varepsilon_2 \ldots \tag{3.2}$$

at fixed m and L. This is observed consistently in Figure 2 (on the left). As we increase the volume at fixed m, more eigenvalues are accumulated near zero, and we infer

$$\varepsilon_i(V_1) > \varepsilon_i(V_2) \qquad \text{for} \quad V_1 > V_2 . \tag{3.3}$$

Also that property is observed consistently from our data, as Figure 2 (on the right) shows.

3.1 Method 1 : Gaussian summation

Our first method to sum over the topologies relies on the assumption that the probability distribution of the charges ν is Gaussian. Indeed general experience shows that possible deviations from a Gaussian distribution tend to be small. Here our assumption implies

$$\Sigma = \sum_{\nu=-\infty}^{\infty} p(|\nu|) \, \Sigma_{|\nu|} , \quad \text{where} \quad p(|\nu|) = \frac{\exp\{-\nu^2/(2V\chi_t)\}}{\sum_\nu \exp\{-\nu^2/(2V\chi_t)\}} ,$$
$$\Sigma_{|\nu|} := -\langle \bar{\psi}\psi \rangle_{|\nu|} \quad \text{and} \quad \chi_t = \langle \nu^2 \rangle/V \quad \text{is the topological susceptibility.} \tag{3.4}$$

Assume we have measured results for $\Sigma_0 \ldots \Sigma_Q$. This constrains the values at all higher charges based on eq. (3.2),

$$\frac{|\nu|}{mV} < \Sigma_{|\nu|} < \frac{|\nu|}{mV} + \varepsilon_Q . \tag{3.5}$$

For $L = 24$ and 28 we also have gaps at low $|\nu|$, where we insert the obvious bounds based on eq. (3.3). Thus we obtain — with remarkably mild uncertainties — the full set of $\Sigma_{|\nu|}$ to be inserted in eq. (3.4). The only unknown parameter is the susceptibility χ_t, which we *tune* so that the sum
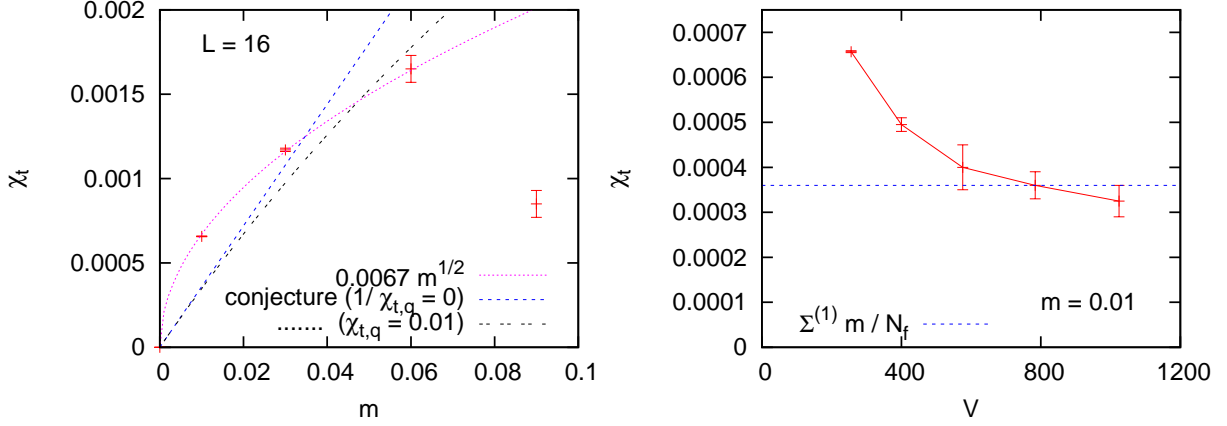
Figure 3: Results for the topological susceptibility χ_t for light fermions, obtained by assuming a Gaussian distribution of the topological charges and matching the theoretical value of Σ. The plot on the left suggests a behaviour $\chi_t \propto \sqrt{m}$ at small masses. The plot on the right shows a nice convergence to the value conjectured in Ref. [16] (in infinite volume), from where we also adapted the quenched susceptibility $\chi_{t,q}$.

reproduces the theoretical Σ value (1.2). Thus we obtain the results for χ_t shown in Figure 3. For very light fermions they suggest $\chi_t \propto \sqrt{m}$ (in a fixed volume), see plot on the left.

Alternative results (with quenched configurations and re-weighting) were given in Ref. [15]. On the theoretical side, Ref. [16] conjectured for N_f degenerate flavours in the large volume limit

$$\frac{1}{\chi_t} = \frac{N_f}{\Sigma^{(1)} m} + \frac{1}{\chi_{t,q}} , \qquad \Sigma^{(1)} := \Sigma_{N_f=1}(m=0) \simeq 0.16 g , \qquad (3.6)$$

where $\chi_{t,q} = \chi_t(m \to \infty)$ is the quenched value. As we increase the volume at $m = 0.01$, our results converge to the vicinity of this prediction, see Figure 3 on the right.
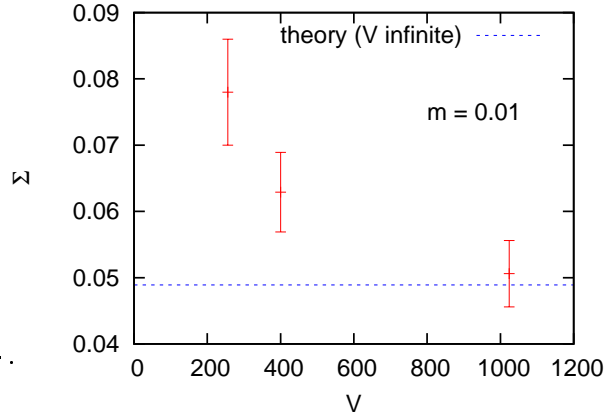
3.2 Method 2 : Summation formula

The first method used the theoretically predicted Σ value as an input to extract χ_t. Now we try to evaluate Σ itself from our data. We apply an approximation formula [12], in exact analogy to a formula for the pion mass derived in Ref. [17],

$$\Sigma_{|v|} \approx \Sigma - \frac{A}{V} + v^2 \frac{B}{V^2} , \quad A = \frac{\alpha}{\chi_t} , \quad B = \frac{\alpha}{\chi_t^2} .$$
$$(3.7)$$

The derivation involves a Fourier transform between v and the vacuum angle θ, which is treated by the stationary phase approximation.

Figure 4: The chiral condensate Σ at $m = 0.01$ as a function of the volume, obtained from measurements of various $\Sigma_{|v|}$ values and the approximate summation formula (3.7).

Formula (3.7) involves three unknown parameters. Two of them, Σ and $\chi_t = A/B$ are of physical interest (unlike α). We capture them if we manage to determine A and B.

5
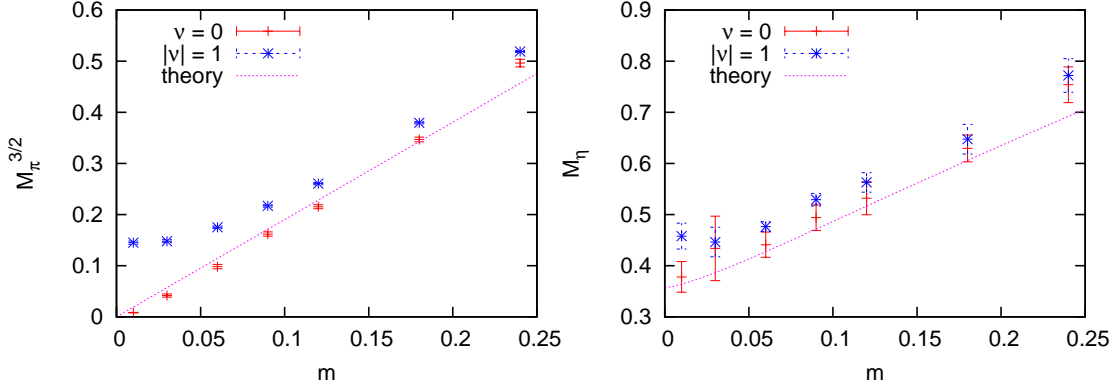
Figure 5: $M_\pi^{3/2}$ and M_η as functions of the fermion mass m at $L = 16$, measured in the sectors $|\nu| = 0$ and 1. For comparison we show the theoretical prediction (summed over all topologies).

- At fixed m and V we can extract B, *e.g.* from Σ_0 and Σ_1.
- At fixed m in two volumes $V_1 \neq V_2$, we can evaluate A, *e.g.* from $\Sigma_0(V_1)$ and $\Sigma_0(V_2)$.

    $\Sigma_{|\nu|}$ values in three volumes determine all three parameters.

    For a combined approach along these lines [12], we arrived at the results for Σ shown in Figure 4. As in Figure 3 (on the right) we see for increasing volume a flow towards the value (1.2), which was predicted theoretically (in infinite volume).

3.3 Method 3 : Density correlation

    A third method has been suggested in Refs. [18]. The derivation is similar to Ref. [17],[1] and it leads to a formula for finite size effects in the correlation of the topological charge density ρ,

$$\langle \rho(x)\rho(y) \rangle_{|\nu|} \rightarrow \frac{1}{V}\left(\frac{\nu^2}{V} - \chi_t - \frac{c_4}{2\chi_t V} \right) + O(V^{-3}) \,. \tag{3.8}$$

(The kurtosis $c_4 = (3\langle \nu^2 \rangle^2 - \langle \nu^4 \rangle)/V$ is a measure for the deviation from a Gaussian charge distribution.) The formula refers to the asymptotic behaviour at large $|x - y|$. This requires a large volume, and unfortunately this also means that the signal to extract χ_t is likely to be too small for a conclusive measurement. Later Ref. [19] considered instead the η'-correlator of the pseudo-scalar density, which obeys the analogous formula, and where a sensible signal was found, even in QCD with dynamical overlap quark. Also in our project this method is under investigation [12].

4. Meson masses

    We measured the "meson masses" based on current correlators, which is most efficient in this model [2], and we show the results for $L = 16$ in Figure 5. At least for $m = 0.01$ we are clearly in the ε-regime. For increasing m the topological distinction shrinks. The masses measured in $|\nu| = 0$ and 1 are compared to the predictions of Refs. [1, 2] (which refer to $m \ll g \simeq 0.45$).

    At last we apply Method 2 to the pion mass, as it was originally intended [17]. We fix $m = 0.01$, $|\nu| = 1$ and employ the formula (3.7), $M_{\pi,1} \approx M_\pi - A/V + B/V^2$. We have results from three

---

[1]In both cases the approximation should be best for small $|\nu|$, so that $\langle \nu^2 \rangle \gg |\nu|$.

volumes, which we insert and solve for M_π,

$$\{ M_{\pi,1}^{(L=16)} = 0.276(4) \,, \ M_{\pi,1}^{(L=20)} = 0.214(4) \,, \ M_{\pi,1}^{(L=32)} = 0.135(4) \} \ \Rightarrow \ M_\pi = 0.078(8) \,. \quad (4.1)$$

This is indeed compatible with the theoretical value in eq. (1.2), $M_\pi = 0.0713\ldots$ Considering the large $M_{\pi,1}^{(L)}$ masses that we started from, this agreement is an impressive success of this method.

5. Conclusions

Based on our experience, it appears possible — at least in some cases — to derive observables, which are properly summed over all topologies, even if only measurements in a few fixed sectors are available. This property (which agrees with Ref. [19]) is crucial for the future of dynamical overlap fermion simulations, in particular in the ε-regime, where topology is essential [20]. The exact results and their reliability depends on subtleties and needs to be explored further — the Schwinger model is ideal for such tests before large-scale QCD applications.

References

[1] A.V. Smilga, *Phys. Rev.* **D 55** (1997) 443.

[2] C. Gattringer, I. Hip and C.B. Lang, *Phys. Lett.* **B 466** (1999) 287.

[3] W. Bietenholz, *Eur. Phys. J.* **C 6** (1999) 537.

[4] W. Bietenholz and I. Hip, *Nucl. Phys.* **B 570** (2000) 423.

[5] H. Neuberger, *Phys. Lett.* **B 417** (1998) 141.

[6] P. Hasenfratz, V. Laliena and F. Niedermayer, *Phys. Lett.* **B 427** (1998) 125.

[7] M. Lüscher, *Phys. Lett.* **B 428** (1998) 342.

[8] D.H. Adams and W. Bietenholz, *Eur. Phys. J.* **C 34** (2004) 245.

[9] N. Christian, K. Jansen, K.-I. Nagai and B. Pollakowski, *Nucl. Phys.* **B 739** (2006) 60.

[10] W. Bietenholz, *Nucl. Phys.* **B 644** (2002) 223. S. Shcheredin, Ph.D. Thesis, Humboldt Universität zu Berlin (2004) [hep-lat/0502001]. W. Bietenholz and S. Shcheredin, *Nucl. Phys.* **B 754** (2006) 17.

[11] J. Volkholz, W. Bietenholz and S. Shcheredin, PoS(LAT2006)040.

[12] W. Bietenholz, I. Hip, S. Shcheredin and J. Volkholz, in preparation.

[13] N. Christian, K. Jansen, K.-I. Nagai and B. Pollakowski, PoS(LAT2005)239.

[14] W. Bietenholz, J. Volkholz and S. Shcheredin, PoS(LAT2007)064.

[15] S. Dürr and C. Hoelbling, *Phys. Rev.* **D 69** (2004) 034503.

[16] S. Dürr, *Nucl. Phys.* **B 611** (2001) 281, and private communication.

[17] R. Brower, S. Chandrasekharan, J.W. Negele and U.-J. Wiese, *Phys. Lett.* **B 560** (2003) 64.

[18] S. Aoki, H. Fukaya, S. Hashimoto and T. Onogi, *Phys. Rev.* **D 76** (2007) 054508.

[19] S. Aoki *et al.* (JLQCD and TWQCD Collaborations), *Phys. Lett.* **B 665** (2008) 294.

[20] H. Leutwyler and A.V. Smilga, *Phys. Rev.* **D 46** (1992) 5607.